Available online at www.sciencedirect.com
ScienceDirect
Journal of Sound and Vibration 320 (2009) 101–124
JOURNAL OF SOUND AND VIBRATION
www.elsevier.com/locate/jsvi

Vibrations of steel–concrete composite beams with partially degraded connection and applications to damage detection

Michele Dilena, Antonino Morassi*

Dipartimento di Georisorse e Territorio, Università degli Studi di Udine, Via Cotonificio 114, 33100 Udine, Italy

Received 13 February 2007; received in revised form 24 July 2008; accepted 27 July 2008
Handling Editor: A.V. Metrikine
Available online 5 September 2008

Abstract

Vibrational methods are frequently used as diagnostic tools to detect damage in structures. One of the main difficulties connected with the use of such methods lies in the small sensitivity of the dynamic parameters to damage. This is an intrinsic feature of structural diagnostics based on dynamic data. It represents a source of important indeterminacy, such as the strong dependence of the results of identification on the experimental errors and on the accuracy of the structural model that is chosen to interpret measurements. Application of dynamic techniques to the case of steel–concrete composite beams, in addition, makes the problem more complicated, owing to the uncertainty about the mechanical behaviour of the connection and damage modelling. Previous research on vibrational methods for damage detection in composite beams was concerned with the identification of severe levels of damage. In this paper we present an Euler–Bernoulli model of composite beam which accurately describes the dynamic response measured on composite beams with either severe or intermediate levels of damage. A diagnostic technique based on frequency measurements is then applied to the suggested model and it gives positive results. A Timoshenko model of composite beam is also derived and used for diagnostic purposes.

1. Introduction

In this paper we continue a line of research initiated in Ref. [1] and aim at the study and development of non-destructive methods for damage detection in steel–concrete composite structures from dynamic test data.

Steel–concrete composite system is widely used in bridge construction and also for long-span building floors, see, for example, Ref. [2]. The global structural behaviour is achieved by shear connectors placed between the concrete slab and the steel beams. Assessment of the connection integrity is obviously of primary importance for evaluating the safety of the system. In ageing bridges, for example, the condition of the connectors may not be good due to the occurrence of corrosion and fatigue phenomena or to unexpected overloading. Failure or even damage of the shear connectors will significantly reduce the composite action and, therefore, reduce the bridge load-carrying capacity. Since the inaccessibility of the connection makes the

*Corresponding author. Tel.: +39 0432 558739; fax: +39 0432 558700.
E-mail addresses: michele_dilena@email.it (M. Dilena), antonino.morassi@uniud.it (A. Morassi).

0022-460X/$ - see front matter © 2008 Elsevier Ltd. All rights reserved.
doi:10.1016/j.jsv.2008.07.022

inspection difficult, it is of practical importance to develop non-destructive techniques to assess the integrity of the connection, see, for instance, Ref. [3].

Within the large class of methods of non-destructive testing, dynamic techniques have received great attention in engineering communities in last decades, see, for example, Refs. [4–7]. In fact, unlike other conventional diagnostic methods, such as radiography, thermal analysis or techniques based on penetrating liquids, which have local character, modal analysis techniques offer potential advantages for damage detection in a global scale.

One attempt to detect damage in steel–concrete composite beams via dynamic methods has been originally developed in Refs. [8,9]. In those papers, a series of composite beams were studied dynamically in laboratory, in both undamaged and damaged states. Vibrational methods were used to calibrate a mechanical model of the system and to localise the damage in the connection. The analysis concerned with *severe levels of damage*, corresponding to the extreme case where concrete surrounding a damaged connector is thoroughly degraded and the connection is fully plasticised. For these levels of damage, the mechanical model proposed in Ref. [9] was able to accurately describe the dynamic behaviour measured during the experiments and, moreover, was successfully used for damage detection purposes.

The main goal of this paper is to fill the gap concerning the mechanical modelling and damage identification for composite beams with partially damaged connection, that is for *intermediate levels of damage*. This aspect is of large importance when non-destructive methods based on dynamic measurements are employed to detect possible damage in structures. In fact, one of the main hindrances to the practical use of these techniques lies in the relatively small sensitivity of the dynamic parameters to damage. This feature of the diagnostic problem reflects into a series of practical difficulties, even in the study of simple systems, such as notched steel beams and frames. In fact, it is well known that the results of most diagnostic techniques strictly depend on the accuracy of the analytical model used for the interpretation of experiments, on the measurement errors and on the damage severity to be identified, see, for example, Refs. [10–12]. Application of these techniques to assess structural integrity of steel–concrete composite beams, in addition, makes the diagnostic problem more involved, owing to the uncertainty about the modelling of the connection and the description of the damage. Therefore, the study of the sensitivity of dynamic parameters to small levels of damage (see Ref. [13]) and the development of accurate analytical models of composite beams with partially degraded connection are central points of the analysis.

In this paper, a dynamic Euler–Bernoulli model of composite beam based on a *shear model* of the connection is proposed for the interpretation of the experimental results carried out in Ref. [13] and for the identification of damage. The model accurately describes the dynamic behaviour observed in the experiments and allows for a rather precise identification of either severe or intermediate damages. In the last section of the paper, the model is refined accordingly to Timoshenko theory and used to improve damage detection results.

2. A shearing-type Euler–Bernoulli model

The analysis developed in this paper will mainly concern with the Euler–Bernoulli model of composite beam presented below. Such a model differs from that defined in Ref. [9] in the expression of the shearing strain energy of the connection. Nevertheless, for the sake of completeness, a brief general introduction to the mechanical model follows.

The quantities relative to the concrete beam and to the steel beam will be denoted by indices $i = 1, 2$, respectively, see Fig. 1. To simplify notation and since the analysis will refer to this particular situation, the case of uniform composite beam will be considered. Let (O_i, X_i, Y_i, Z_i), $i = 1, 2$, be a Cartesian coordinate system whose origin O_i coincides with the barycentre G_i of the ith transversal cross-section. The axes X_i, Y_i, $i = 1, 2$, agree with the inertia principal directions of the ith transversal cross-section at G_i, $i = 1, 2$. It is assumed that the two axes Y_i, $i = 1, 2$, coincide with the same vertical direction Y and are oriented downwards. The axes Z_i, $i = 1, 2$, define the direction Z of the longitudinal axis of each beam and they run parallel at a distance e. The following analysis will consider the small free vibrations of the connected system in the vertical plane $Y - Z$ around a straight and not stressed equilibrium state.

The two beams forming the system can slide at the steel–concrete interface. Relative transversal displacements between the two beams are allowed. As a consequence, in accordance with the Euler–Bernoulli

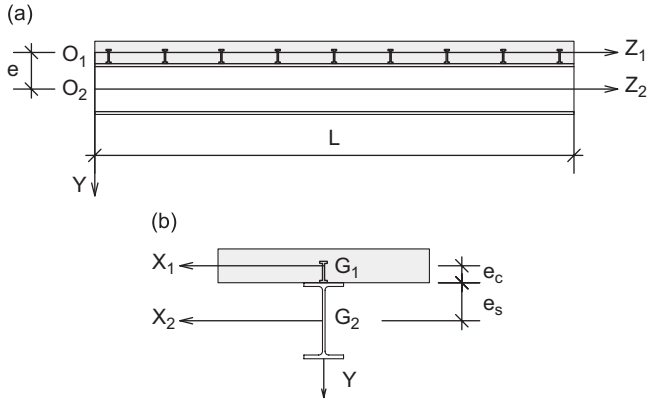

Fig. 1. Steel–concrete composite beam: (a) longitudinal view; (b) transversal cross-section.

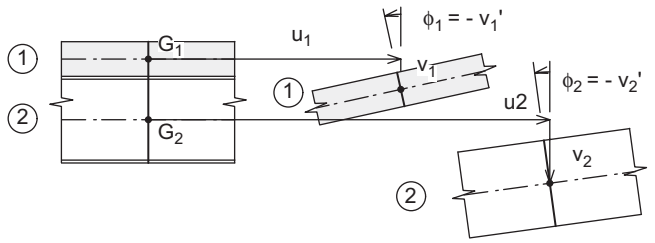

Fig. 2. Displacements and rotational fields for the Euler–Bernoulli model.

theory of beams, the actual configuration of the system is described by assigning the axial displacements $u_i(z,t)$, $i=1,2$, and transversal displacements $v_i(z,t)$, $i=1,2$, of z abscissa's transversal section at a moment of time t, see Fig. 2. Under the assumption of linear elastic constitutive equations and of homogeneous isotropic materials, the strain energy stored in the two beams at time t is given by

$$V_b(t)=\sum_{i=1}^{2}\frac{1}{2}\int_0^L\left(a_i\left(\frac{\partial u_i}{\partial z}\right)^2+j_i\left(\frac{\partial^2 v_i}{\partial z^2}\right)^2\right)\mathrm{d}z, \tag{1}$$

where L is the length of the composite beam, $a_i\equiv E_iA_i$ and $j_i\equiv E_iJ_i$ are the axial stiffness and the bending stiffness of the ith beam, $i=1,2$. The quantities A_i and J_i are the area and the moment of inertia (evaluated with respect to the axis X_i) of the ith cross-section and E_i is Young's modulus of the material.

Regarding modelling of the connection, a rigorous definition of the strain energy, even in the simple case of undamaged state, would involve a detailed study of the three-dimensional interaction effects between the connectors and the surrounding concrete. A full analysis of these effects is beyond the goals of this research and, however, it would be extremely difficult to include in a mechanical model of reduced dimension. In Ref. [9] a one-dimensional model for the case of *undamaged system* was proposed, see also Ref. [1]. Each stud was ideally modelled as an *equivalent beam*, whose bottom and top ends were fixed to the steel beam flange and to the concrete slab axis, respectively. Considering that the distance between two consecutive studs is short with respect to the beam length, the strain energy in the connection was described in terms of an interface energy density. This density function was the sum of three contributions: one relative to sliding in longitudinal direction Z between the base and the head of the connector (*shearing-type energy*); a second term is due by the occurrence of rotations at both ends of each connector (*rotational-type energy*); the last contribution comes from the relative transversal displacement in Y direction (*axial-type energy*), see Ref. [9, Section 2] for more details. This mechanical model proved to be accurate for the interpretation of the dynamic tests carried out by Morassi and Rocchetto [8].

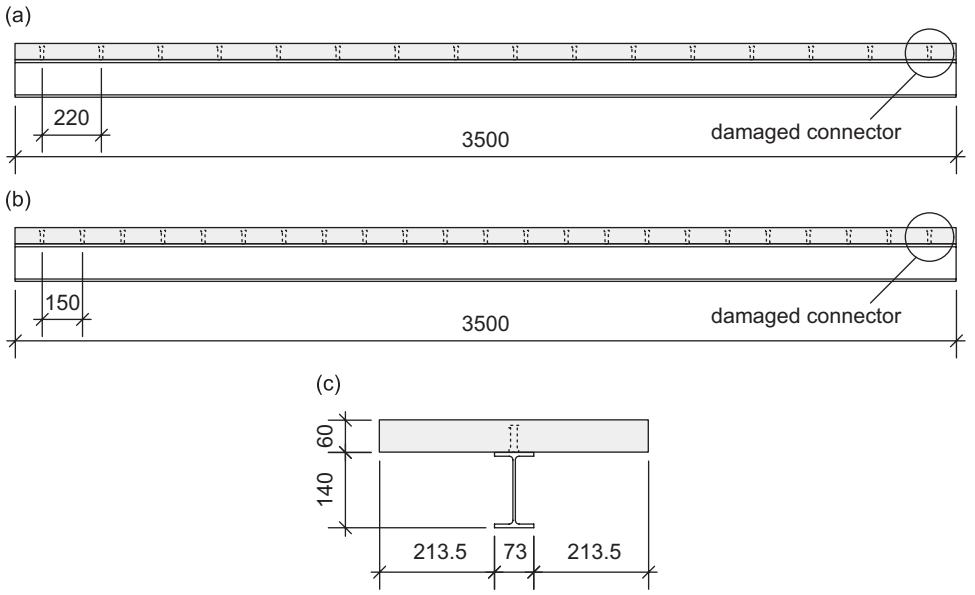

Fig. 3. Steel–concrete composite beams investigated in experiments (see Ref. [13]): front view of (a) T1PR beam (partial connection) and (b) T1CR beam (total connection); (c) transversal section. Lengths in millimetres.

In Ref. [14] a slightly different model of undamaged composite beam was introduced, including other coupling terms in the strain energy of the connection. The analytical results obtained in Ref. [14], compared with the experimental findings found in Refs. [1,8], essentially show no significant improvement in the accuracy with respect to the model developed in Ref. [9].

It is worth noticing that all the above mechanical models were tested on the *undamaged* composite beams studied in the experiments carried out in Refs. [1,8], see Fig. 3. The thickness of the concrete slab (60 mm) of these specimens is very short with respect to the length of the connectors (about 50 mm), and this special geometry supports the *equivalent beam* model for the description of the connectors. Conversely, the thickness of the slab is significantly greater than the stud length in several cases of practical interest, see Ref. [2]. Therefore, the equivalent beam model is not suitable for describing the actual strain energy of the connection. In such cases, in fact, the interaction between studs and surrounding concrete is confined to a small region of the slab near the steel–concrete interface and a different strain energy function of the connection must be introduced.

Taking into account these considerations and with a viewpoint on real applications, the *shearing-type model* of the connection has been adopted in this paper, see Refs. [15–21] for applications of a similar mechanical model to composite beams under static loads. Moreover, as in Ref. [9], the *axial strain energy* of the connection due to the possible occurrence of relative transversal displacements is taken into account, see also Ref. [16]. Summing up, the strain energy of the connection of the present model is assumed as

$$V_c(t) = \int_0^L \frac{1}{2} k \left(u_2 - u_1 + e_c \frac{\partial v_1}{\partial z} + e_s \frac{\partial v_2}{\partial z} \right)^2 \mathrm{d}z + \int_0^L \frac{1}{2} \mu (v_2 - v_1)^2 \mathrm{d}z. \tag{2}$$

In Eq. (2), $k = k(z)$ and $\mu = \mu(z)$ are, respectively, the *shearing* and the *axial* stiffness per unit length of the connection. The quantity e_c denotes the distance between the barycentre of the slab and the steel–concrete interface, whereas e_s is the distance between the barycentre of the steel beam and its top flange, see Fig. 1. The first integral in the right-hand side of Eq. (2) is defined in terms of the global sliding $(u_2 - u_1 + e_c \partial v_1/\partial z + e_s \partial v_2/\partial z)$ along Z longitudinal direction occurring at the interface of the two materials, under the Euler–Bernoulli kinematic hypothesis, see Fig. 2. The second contribution represents the strain energy due to the relative transversal displacement $(v_2 - v_1)$.

Now, by adapting the arguments used in Ref. [9], the case of *damaged* connection can be also included in the model. In this case, the stiffness coefficients k, μ in Eq. (2) are replaced by their damaged values k_d, μ_d, which, for one end connector, are assumed to have the following expressions:

$$\begin{aligned} k_d(z) &= k(z)(\chi_{(0,L-d)}(z) + \varphi\chi_{(L-d,L)}(z)), \\ \mu_d(z) &= \mu(z)(\chi_{(0,L-d)}(z) + \psi\chi_{(L-d,L)}(z)). \end{aligned} \tag{3}$$

In Eq. (3), $\chi_I(z)$ is the characteristic function of the interval I, $I \subset (0, L)$, e.g. $\chi_I(z) = 1$ if $z \in I$ and $\chi_I(z) = 0$ if $z \in (0, L)\backslash I$. Moreover, d is the length of the damaged zone and the quantities φ, ψ are two non-dimensional parameters which express the severity of the damage, with $0 \leqslant \varphi \leqslant 1$, $0 \leqslant \psi \leqslant 1$. The values $\{\varphi = 1, \psi = 1\}$ determine the undamaged state, whereas the pair $\{\varphi = 0, \psi = 0\}$ defines the most severe level of damage. The latter corresponds to the extreme case where the connector cannot hinder relative longitudinal and transversal displacements between the slab and the metallic beam. The *intermediate levels of damage* correspond to pairs $\{\varphi, \psi\}$ such that $0 < \varphi < 1$, $0 < \psi < 1$. In Section 3, a procedure for estimating φ, ψ from dynamic measurements on damaged beams will be suggested.

Finally, the dynamic behaviour of the composite system is completed by assigning the expression of its kinetic energy $T(t)$. Neglecting the influence of the rotation of the beam transversal sections, we have

$$T(t) = \sum_{i=1}^{2} \frac{1}{2} \int_0^L \rho_i \left(\left(\frac{\partial u_i}{\partial t} \right)^2 + \left(\frac{\partial v_i}{\partial t} \right)^2 \right) \mathrm{d}z, \tag{4}$$

where ρ_i is the linear mass density of the ith beam. For vibrations that are harmonic in time with radian frequency ω,

$$u_i(z, t) = u_i(z) \cos \omega t, \quad v_i(z, t) = v_i(z) \cos \omega t, \tag{5}$$

$i = 1, 2$, the spatial variation of the free vibrations can be obtained by imposing the stationarity of the Rayleigh quotient of the system under a suitable set of admissible configurations, see Ref. [22]. To fix ideas and considering that experiments have been carried out on free–free beams, this set of boundary conditions will be closely examined in the following. Therefore, the free vibrations are governed by the following system of ordinary differential equations:

$$\begin{cases} N_1' + k_d(u_2 - u_1 + e_c v_1' + e_s v_2') + \omega^2 \rho_1 u_1 = 0, \\ N_2' - k_d(u_2 - u_1 + e_c v_1' + e_s v_2') + \omega^2 \rho_2 u_2 = 0, \\ T_1' + \mu_d(v_2 - v_1) + \omega^2 \rho_1 v_1 = 0, \\ T_2' - \mu_d(v_2 - v_1) + \omega^2 \rho_2 v_2 = 0, \end{cases} \tag{6}$$

in $(0, L - d) \cup (L - d, L)$. Here, the symbol $(\,)'$ means first derivative with respect to the spatial variable z. The *axial forces* $N_i = N_i(z)$ and the *shear forces* $T_i = T_i(z)$, $i = 1, 2$, are given by

$$\begin{aligned} N_i &= a_i u_i', \quad i = 1, 2, \\ T_1 &= M_1' - k_d(u_2 - u_1 + e_c v_1' + e_s v_2')e_c, \\ T_2 &= M_2' - k_d(u_2 - u_1 + e_c v_1' + e_s v_2')e_s \end{aligned} \tag{7}$$

and

$$M_i = -j_i v_i'', \quad i = 1, 2 \tag{8}$$

are the *bending moments*. The differential system of Eq. (6) is completed by the assignment of the jump conditions

$$\begin{aligned} &[u_i(L - d)] = [v_i(L - d)] = [v_i'(L - d)] = 0, \quad i = 1, 2, \\ &[N_i(L - d)] = [T_i(L - d)] = [M_i(L - d)] = 0, \quad i = 1, 2, \end{aligned} \tag{9}$$

where $[f(L - d)] \equiv f((L - d)^+) - f((L - d)^-)$, and by the boundary conditions

$$N_i(z) = T_i(z) = M_i(z) = 0, \quad i = 1, 2 \quad \text{at } z = 0 \text{ and } z = L. \tag{10}$$

The eigenvalue problem defined by Eqs. (6)–(10) can be solved in exact form for the undamaged system and for damaged composite beams with stepwise constant coefficients see Refs. [9,23] for a comprehensive analytical and numerical study. Generally speaking, a prevalence of transversal displacements (*flexural vibrations*) or longitudinal displacements (*axial vibrations*) has been observed from the analysis of the first lower modes. Conversely, the coupling between transversal and longitudinal vibrations increases as the mode order rises.

3. Model calibration for composite beams with partially damaged connection

The model defined by Eqs. (6)–(10) will be used in this section to interpret the dynamic tests on composite beams under severe and intermediate levels of damage. In particular, the experimental results obtained for T1PR and T1CR specimens of Ref. [13] will be closely interpreted, see Fig. 3. The other pair of samples considered in those experiments revealed no substantial new elements. As it is shown in Fig. 4, damage corresponds to a symmetric notch of increasing depth induced by saw-cutting the base of the right-end connector of the composite beam. Each damage configuration was obtained firstly by removing concrete around the connector by using a cylindrical hole (80 mm diameter) and punching it all through the slab with a rotating tool. Subsequently, the concrete surrounding the stud was broken and removed. Then, the connector was saw-cut at the wished depth by means of a controlled cog-rotating wheel. Filling the hole with a suitable mortar mixture finally restored the solidarity between the r.c. slab and the connector. All the dynamic tests were carried out only when the mortar mixture was completely cured (at least 1 month after filling).

Dynamic tests were performed by using an impulsive technique. Each beam was suspended by two steel wire ropes to simulate free–free boundary conditions. Concerning flexural vibrations, the beam was excited transversally and measurement of the transversal response was taken on one end section of the concrete slab by a piezoelectric accelerometer. The modal components of the flexural modes were measured exciting transversally on the slab extrados and on the flange intrados of the steel beam, at 21 orderly spaced points along the beam axis. The frequency response function inertance was measured and natural frequencies and mode shapes were extracted by means of a suitable curve-fitting algorithm; see Ref. [13] for a complete account of the experiment. This measurement set-up was maintained also for all the damage configurations considered in experiments. It was shown in Ref. [13] that the perturbation of the specimen due to the execution of the damage has negligible effect on first two flexural modes and causes an error on higher frequencies which is—in absolute value—at most of order 0.8% and 0.3% for beams with partial and total connection, respectively.

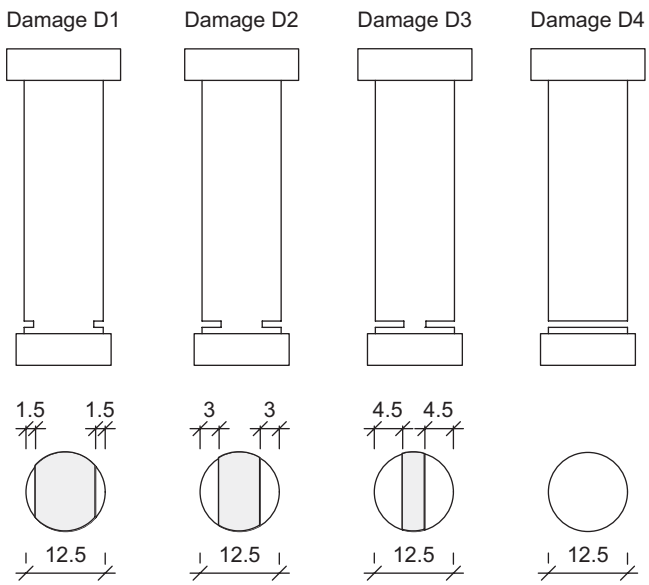

Fig. 4. Damage scenarios (from Ref. [13]). Length in millimetres.

Frequency-induced changes that are below these threshold values may not be reliable for dynamic characterization and damage assessment, since they could be masked by the perturbation of the specimen.

The model described by Eqs. (6), with $\varphi = \psi = 1$ and boundary conditions as in Eq. (10), was used for the interpretation of dynamic tests on undamaged beams. The mechanical and inertial coefficients of the slab and the metallic beam were assumed equal to the values shown in Table 1. Young's modulus E_1 of the concrete was taken equal to the origin tangent mean value $E_1 = 42,863\,\text{MPa}$ deduced in a series of single-axle compressive stress tests performed on some material samples prepared during slab casting.

The values of the axial and shearing stiffness of the connection were determined according to the following identification procedure based on dynamic data. A numerical study shows that the sensitivity of the (flexural) vibration modes to uniform changes in axial stiffness increases with the mode order, see Fig. 5. Therefore, since available data concern only the first four modes of vibration, the axial stiffness was determined in order to minimise the Euclidean distance between the theoretical and the experimental fourth modes. More precisely, starting from given nominal values μ_0, k_0 of the parameters, the optimal value of the axial stiffness was evaluated by solving the following minimum problem:

$$\text{to find } \mu^{\text{opt}} \text{ such that } \quad F(k_0, \mu_{\text{opt}}) = \min_{0<\mu<2\mu_0} F(k_0, \mu), \tag{11}$$

where

$$F(k_0, \mu) = (|\mathbf{v}_1^{\text{exp}} - \mathbf{v}_1^{\text{anal}}(k_0, \mu)|^2 + |\mathbf{v}_2^{\text{exp}} - \mathbf{v}_2^{\text{anal}}(k_0, \mu)|^2)^{1/2} \tag{12}$$

and $\mathbf{v}_i^{\text{exp}} = (v_i^{\text{exp}}(z_1), \ldots, v_i^{\text{exp}}(z_M))$, $\mathbf{v}_i^{\text{anal}} = (v_i^{\text{anal}}(z_1), \ldots, v_i^{\text{anal}}(z_M))$, $i = 1, 2$, are the experimental and the analytical values of the fourth mode components evaluated at the points $z_1, \ldots, z_M$ of the measurement grid. Points in which the differences between experimental and analytical components are very large (typically the two end points) were excluded from the expression of the objective function. The nominal value of the axial

Table 1
Physical parameters of the composite beams T1PR and T1CR tested in the experiments: (a) origin tangent value determined by single-axle compressive stress tests on cylinders; (b) 30% of the mean secant value of the ultimate shearing resistance of the connectors, determined by push-out tests (data from Refs. [8,13])

Parameter	Value
Concrete slab	
Length L	3.50 m
Cross-sectional area A_1	$3.00 \times 10^{-2}\,\text{m}^2$
Moment of inertia J_1	$9.00 \times 10^{-6}\,\text{m}^4$
Linear mass density ρ_1 (T1PR)	73.2 kg/m
Linear mass density ρ_1 (T1CR)	77.2 kg/m
Young's modulus $E_1^{(a)}$	42,863 MPa
Steel beam	
Length L	3.50 m
Cross-sectional area A_2	$1.64 \times 10^{-3}\,\text{m}^2$
Moment of inertia J_2	$5.41 \times 10^{-6}\,\text{m}^4$
Linear mass density ρ_2	12.9 kg/m
Young's modulus E_2	210,000 MPa
Shearing and axial stiffness	
Nominal shearing stiffness $k_0^{(b)}$ (T1PR)	$0.936 \times 10^9\,\text{N/m}^2$
Nominal shearing stiffness $k_0^{(b)}$ (T1CR)	$1.346 \times 10^9\,\text{N/m}^2$
Identified shearing stiffness k (T1PR)	$1.216 \times 10^9\,\text{N/m}^2$
Identified shearing stiffness k (T1CR)	$1.963 \times 10^9\,\text{N/m}^2$
Identified axial stiffness μ (T1PR)	$2.749 \times 10^9\,\text{N/m}^2$
Identified axial stiffness μ (T1CR)	$3.952 \times 10^9\,\text{N/m}^2$

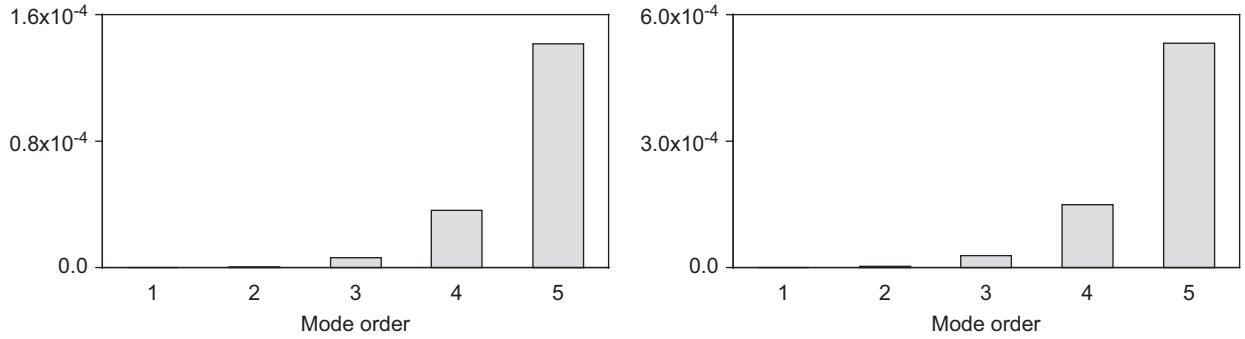

Fig. 5. Natural frequency sensitivity ($\partial\omega^2/\partial\mu$) of the first five (flexural) vibration modes to uniform changes in axial stiffness of the connection evaluated for nominal values (left) and identified values (right) of the parameters μ, k.

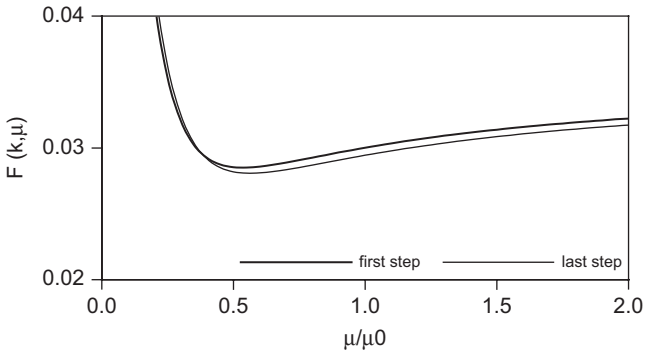

Fig. 6. Error function F of Eq. (12) (T1PR beam).

stiffness was evaluated via the analytical expression derived in Ref. [9] (Eq. (A.3)), namely

$$\mu_0 = \frac{10}{7}\frac{E_c A_c/e_c}{\Delta}, \tag{13}$$

where $e_c = 30\,\text{mm}$ and $E_c = 210,000\,\text{MPa}$, $A_c = 123\,\text{mm}^2$ are Young's modulus and the cross-sectional area, respectively. The length $\Delta = L/n_p$ is the distance between any two equidistant studs, that is $\Delta = 220\,\text{mm}$, $\Delta = 150\,\text{mm}$ for specimens T1PR, T1CR, respectively, see Fig 3. The shearing stiffness nominal value k_0 shown in Table 1 was taken equal to the 30% of the ultimate shearing resistance K_0 of a connector resulting from some push-out tests on samples, see Ref. [9]:

$$k_0 = \frac{K_0}{\Delta}. \tag{14}$$

The graph of the error function F (for fixed shearing stiffness) shows a single global minimum corresponding to a value of the axial stiffness less than the nominal one, see Fig. 6.

Once the axial stiffness was estimated, the shearing stiffness was determined by imposing that the analytical and the experimental frequencies associated to the fundamental mode coincide. The procedure was iterated until negligible changes of the two parameters were obtained in subsequent steps. Typically, convergence was achieved in two or three steps. It turns out that the optimal values of k are $1.30k_0$, $1.46k_0$ for the T1PR and T1CR beam, respectively, whereas the optimal value of μ is equal to $0.50\mu_0$.

Columns 2–4 of Tables 2 and 3 compare, respectively, experimental and analytical frequencies of flexural vibration modes for T1PR and T1CR beams in undamaged configuration. The Euler–Bernoulli model overestimates the measured frequencies and discrepancies are even higher as the mode order rises, following a pattern similar to that of single homogeneous beam having equal slenderness. For the sake of completeness, a

Table 2
Comparison between experimental and analytical frequencies (Euler–Bernoulli model) of flexural vibration modes for T1PR beam in undamaged and damaged configurations (rigid motions are omitted)

Mode	Undamaged			Damage D1			Damage D2			Damage D3			Damage D4		
	Exp.	Anal.	Δ%	Exp.	Anal.	Δ%	Exp.	Anal.	Δ%	Exp.	Anal.	Δ%	Exp.	Anal.	Δ%
1	60.68	60.68	0.0	60.51	60.54	0.0	60.25	60.37	0.2	60.21	60.35	0.2	59.81	60.20	0.7
2	145.46	149.55	2.8	144.08	148.62	3.2	142.70	147.47	3.3	142.18	147.23	3.6	136.76	145.19	6.2
3	247.11	265.25	7.3	245.14	262.86	7.2	241.93	259.78	7.4	238.95	258.68	8.3	222.58	247.68	11.3
4	351.08	401.87	14.5	348.72	398.07	14.2	343.62	392.89	14.3	339.22	389.83	14.9	309.10	357.61	15.7
5	461.38	553.89	20.1	457.49	549.20	20.0	452.41	542.11	19.8	447.98	536.00	19.6	402.96	480.27	19.2
6	570.77	713.32	25.0	565.91	708.31	25.2	560.31	699.78	24.9	554.64	690.39	24.5	503.66	624.68	24.0
7	691.48	873.28	26.3	686.11	868.29	26.6	679.84	858.63	26.3	673.37	846.92	25.8	599.82	774.68	29.2

Identified values of the damaged parameters φ and ψ as in Table 5. $\Delta\% = 100(f_{\text{anal}} - f_{\text{exp}})/f_{\text{exp}}$. Frequency values in Hertz. Experimental data from Ref. [13].

Table 3
Comparison between experimental and analytical frequencies (Euler–Bernoulli model) of flexural vibration modes for T1CR beam in undamaged and damaged configurations (rigid motions are omitted)

Mode	Undamaged			Damage D1			Damage D2			Damage D3			Damage D4		
	Exp.	Anal.	Δ%	Exp.	Anal.	Δ%	Exp.	Anal.	Δ%	Exp.	Anal.	Δ%	Exp.	Anal.	Δ%
1	60.49	60.49	0.0	60.37	60.42	0.1	60.30	60.39	0.2	60.29	60.39	0.2	60.24	60.33	0.2
2	146.34	153.23	4.7	145.12	152.60	5.2	144.80	152.37	5.2	143.97	152.28	5.8	144.30	151.48	5.0
3	250.82	275.03	9.7	248.18	273.04	10.0	246.05	272.31	10.7	245.60	271.84	10.7	242.46	267.31	10.2
4	361.26	418.23	15.8	357.09	414.50	16.1	356.18	413.13	16.0	353.42	411.71	16.5	346.21	396.06	14.4
5	473.88	577.13	21.8	471.08	572.03	21.4	468.00	570.11	21.8	466.29	567.02	21.6	451.06	531.17	17.8
6	588.38	745.49	26.7	586.28	739.46	26.1	583.34	737.18	26.4	580.71	731.83	26.0	560.88	676.51	20.6
7	709.04	915.75	29.2	708.14	909.59	28.4	703.65	907.18	28.9	700.58	899.60	28.4	668.07	835.07	25.0

Identified values of the damaged parameters φ and ψ as in Table 5. $\Delta\% = 100(f_{\text{anal}} - f_{\text{exp}})/f_{\text{exp}}$. Frequency values in Hertz. Experimental data from Ref. [13].

Table 4
Comparison between experimental and analytical natural frequencies of flexural vibration modes (rigid vibration modes are omitted) for T1PR and T1CR beam in undamaged configuration

Mode	Exp. value	Shearing-type model	Δ(%)	Model in Ref. [9]	Δ(%)
T1PR beam					
1	60.68	60.68	0.0	60.68	0.0
2	145.46	149.55	2.8	137.43	−5.5
3	247.11	265.25	7.3	243.21	−1.6
4	351.08	401.87	14.5	373.14	6.3
5	461.38	553.89	20.1	521.04	12.9
6	570.77	713.32	25.0	678.24	18.8
7	691.48	873.28	26.3	837.18	21.1
T1CR beam					
1	60.49	60.49	0.0	60.49	0.0
2	146.34	153.23	4.7	136.47	−6.7
3	250.82	275.03	9.7	241.65	−3.7
4	361.26	418.23	15.8	372.09	3.0
5	473.88	577.13	21.8	523.22	10.4
6	588.38	745.49	26.7	687.90	16.9
7	709.04	915.75	29.2	858.22	17.4

$\Delta\% = 100(f_{\text{anal}} - f_{\text{exp}})/f_{\text{exp}}$. Frequency values in Hertz. Experimental data from Ref. [13].

comparison with the mechanical model proposed in Ref. [9] is presented in Table 4. It can be seen that the accuracy of the two models is quite similar. In addition, the *shearing-type* Euler–Bernoulli model avoids the anomalous underestimate of the second and third frequencies predicted by the previous model. The first four experimental flexural modes are reproduced with high accuracy, see, for example, Fig. 7 for T1PR beam.

The calibrated model is used as a baseline to define the mechanical model of *damaged* composite beam. Once again, reference is made to the experimental results obtained in Ref. [13] for the two specimens T1PR and T1CR. The damage was simulated by means of a crack of increasing depth produced on the right-end connector, see Figs. 3 and 4. The interpretation of dynamic tests on damaged beams is based on the model described by Eqs. (6), jump conditions (9) and boundary conditions (10). Putting $d = 0.25$ and 0.18 m as length of the damaged region for T1PR and T1CR, respectively, it is evident that an accurate description of the dynamic behaviour of composite beam with partially damaged connection requires a careful choice of the unknown parameters k_d and μ_d or, equivalently, of φ and ψ, in Eq. (3). In this analysis, no attempt is made to express the values φ, ψ in terms of the real damage present at the damaged connector. This would require a detailed knowledge of degradation, which is often unavailable in advance in inverse analysis. Therefore, the unknown parameters are identified from frequency shifts measured between undamaged and damaged configurations.

As a preliminary stage, a parametric investigation of the sensitivity of the first flexural frequencies to connection damage parameters φ and ψ has been carried out in Ref. [23]. In particular, Fig. 8 shows the relative variations of the first six frequencies expressed in terms of the parameter φ, for a discrete set of fixed values of ψ. By reversing the role of φ and ψ, similar plots are obtained in Fig. 9. It can be observed that the first and the second frequencies are weakly affected by even large variations of ψ, while they are rather sensitive to variations of the shearing damaged parameter φ. On the contrary, frequency variations associated to higher-order modes almost exclusively depend on the axial stiffness degradation.

As for damage parameter identification, recourse to a variational method based on measurements of the first natural frequencies has been done. Generally speaking, the idea, as one will see briefly, is to look for optimum values of the parameters so as to reduce an error function defined by the differences between the theoretical and the measured frequency values. It is well known that results of these variational approaches are

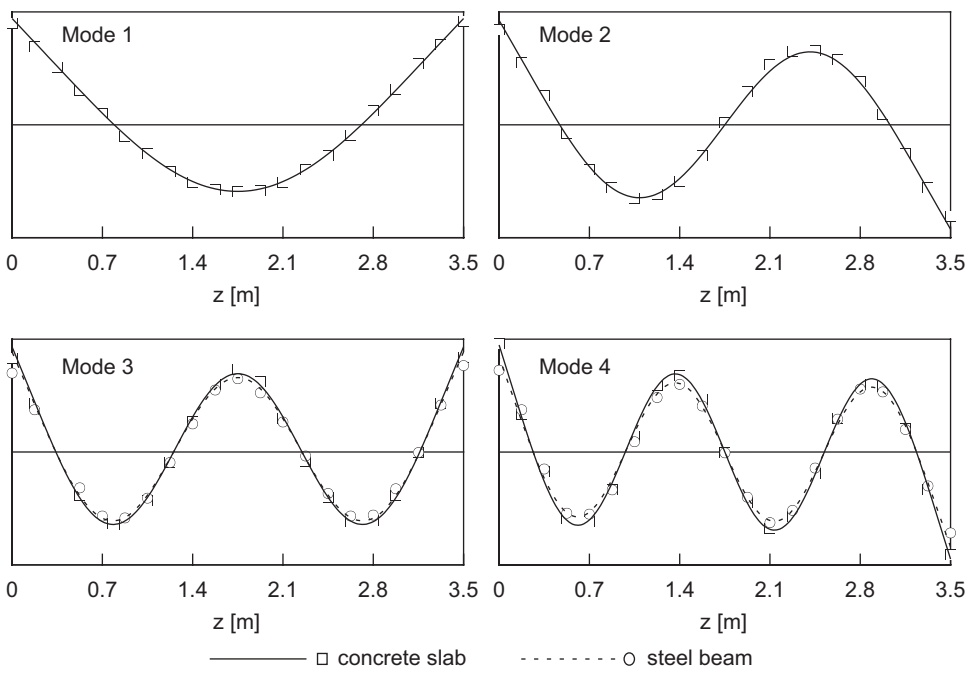

Fig. 7. Comparison between the first four analytical and experimental (dots) flexural modes of T1PR beam in undamaged configuration. Experimental data from Ref. [13].

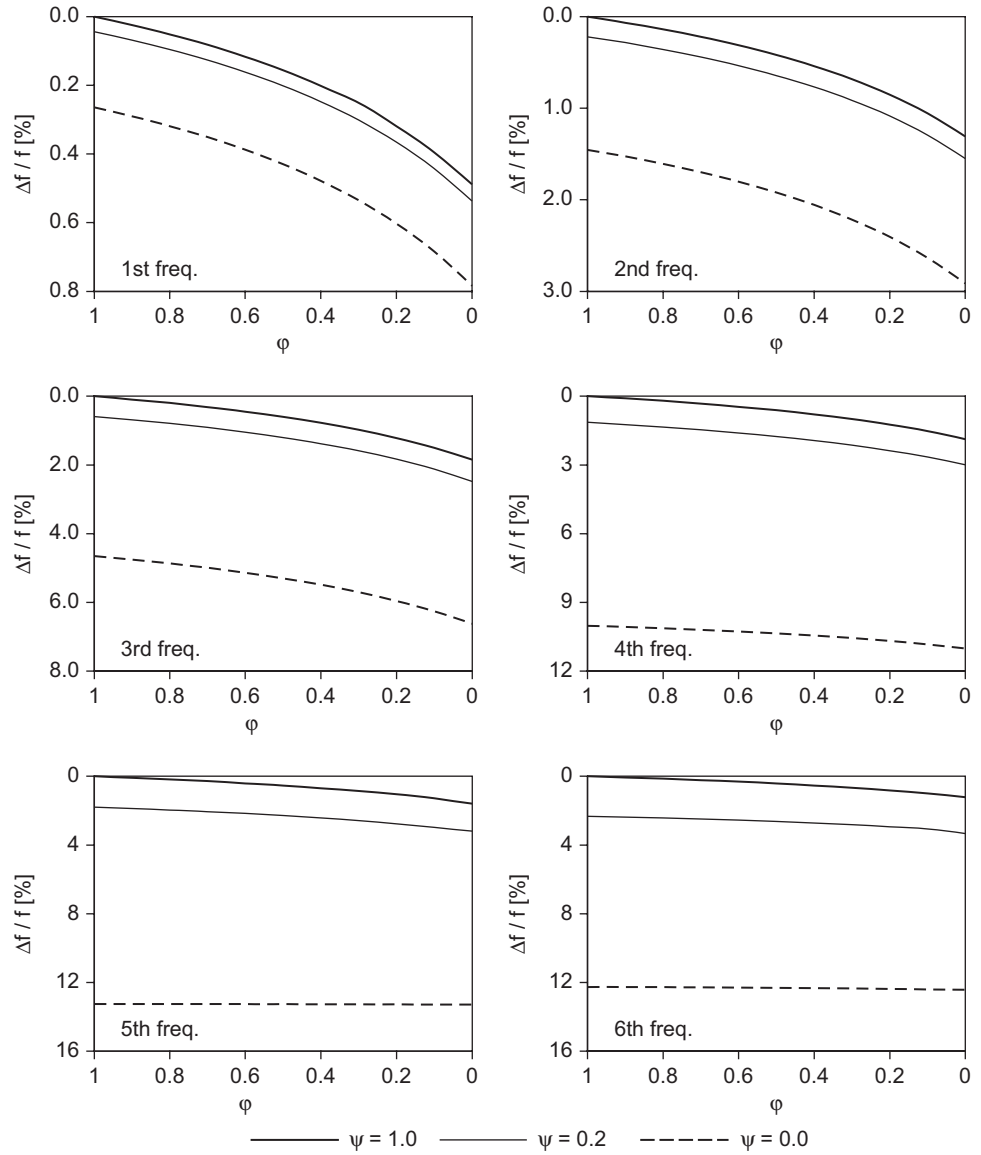

Fig. 8. Percentage variations of the first six flexural frequencies of the T1PR beam (Euler–Bernoulli model) versus shearing stiffness ratio $\varphi \equiv k_d/k$, for different values of axial stiffness ratio $\psi \equiv \mu_d/\mu$.

strongly conditioned by the choice of the error function to be minimised. Therefore, various choices of the error function have been taken into consideration in the analysis.

In a first stage, the error function has been taken to coincide with the Euclidean norm of the distance between the first N experimental frequencies and their analytical counterparts, namely

$$\ell_1(\varphi,\psi) = \sum_{r=1}^{N} \left(\frac{f_{r,\mathrm{exp}} - f_{r,\mathrm{anal}}(\varphi,\psi)}{f_{r,\mathrm{exp}}} \right)^2. \tag{15}$$

In Eq. (15), $f_{r,\mathrm{exp}}$ and $f_{r,\mathrm{anal}}(\varphi,\psi)$ are the experimental and the analytical values of the rth frequency in damage state, respectively. Then, the damage identification problem can be formulated as follows:

$$\text{to find } (\widetilde{\varphi},\widetilde{\psi}) \text{ such that } \ell_1(\widetilde{\varphi},\widetilde{\psi}) = \min_{(\varphi,\psi)\in[0,1]\times[0,1]} \ell_1(\varphi,\psi). \tag{16}$$

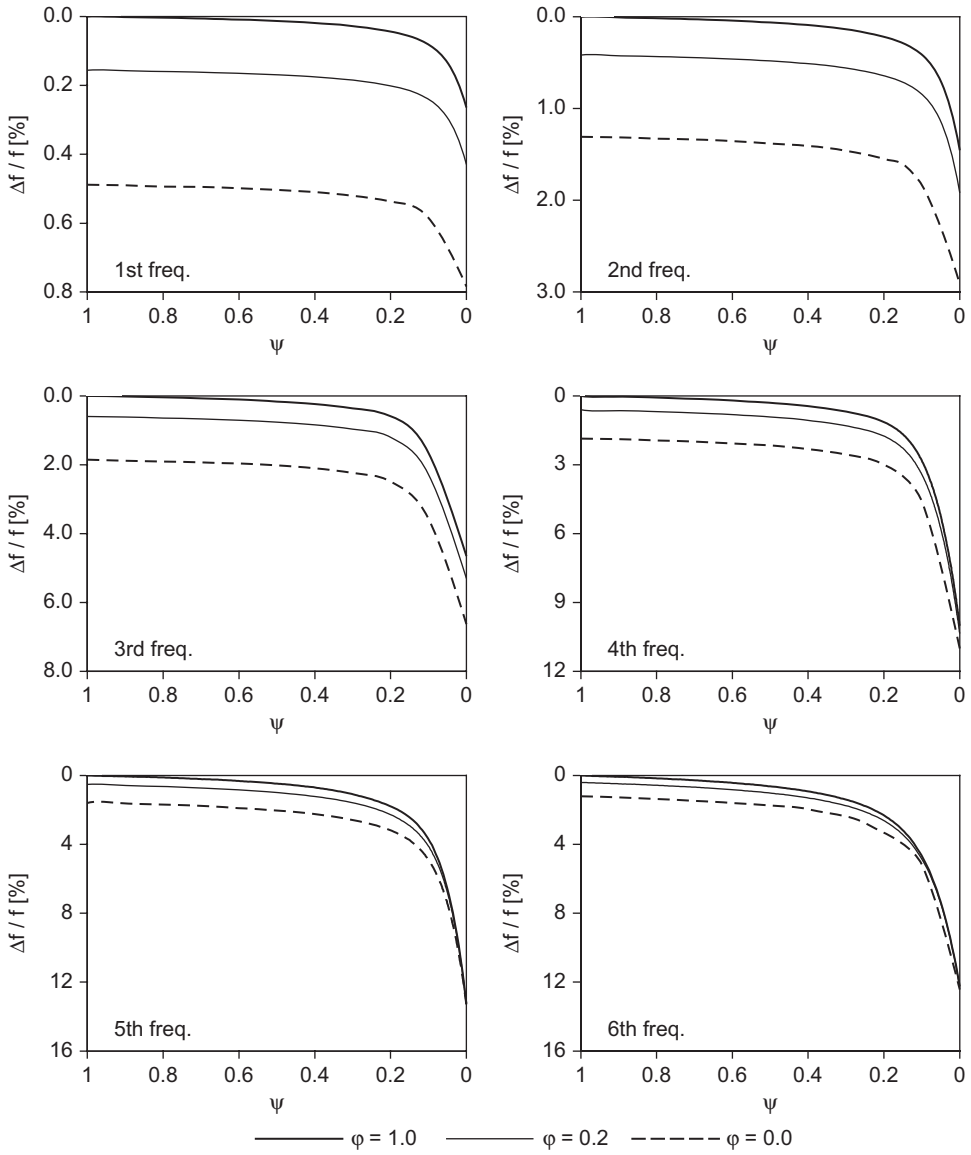

Fig. 9. Percentage variations of the first six flexural frequencies of the T1PR beam (Euler–Bernoulli model) versus axial stiffness ratio $\psi \equiv \mu_d/\mu$, for different values of shearing stiffness ratio $\varphi \equiv k_d/k$.

Fig. 10 shows the typical trend of the surface error which is met in the studied cases. For this objective function choice, the optimum value has turned out coinciding with vanishing values of both parameters of damage for all the damage configurations and for $N = 4, 5, 6$. A possible justification of this result is to be searched in the trend of the modelling errors produced by the analytical model of composite beam used for the interpretation of the measurements. In fact, from Tables 2 and 3 one can see that the analytical model overestimates all the experimental frequencies and modelling errors, assumed uniform in the various damage configurations, grow raising as the mode order increases. Moreover, a detailed analysis of the numerical values reveals that the set of frequencies predicted by the analytical model in the most severe configuration of damage (D4) is the closest one to the experimental values for all the damage configurations. Therefore, it is evident that the variational approach based on the error function of Eq. (15) leads to null values for the damage parameters φ, ψ and the identification turns out completely compromised.

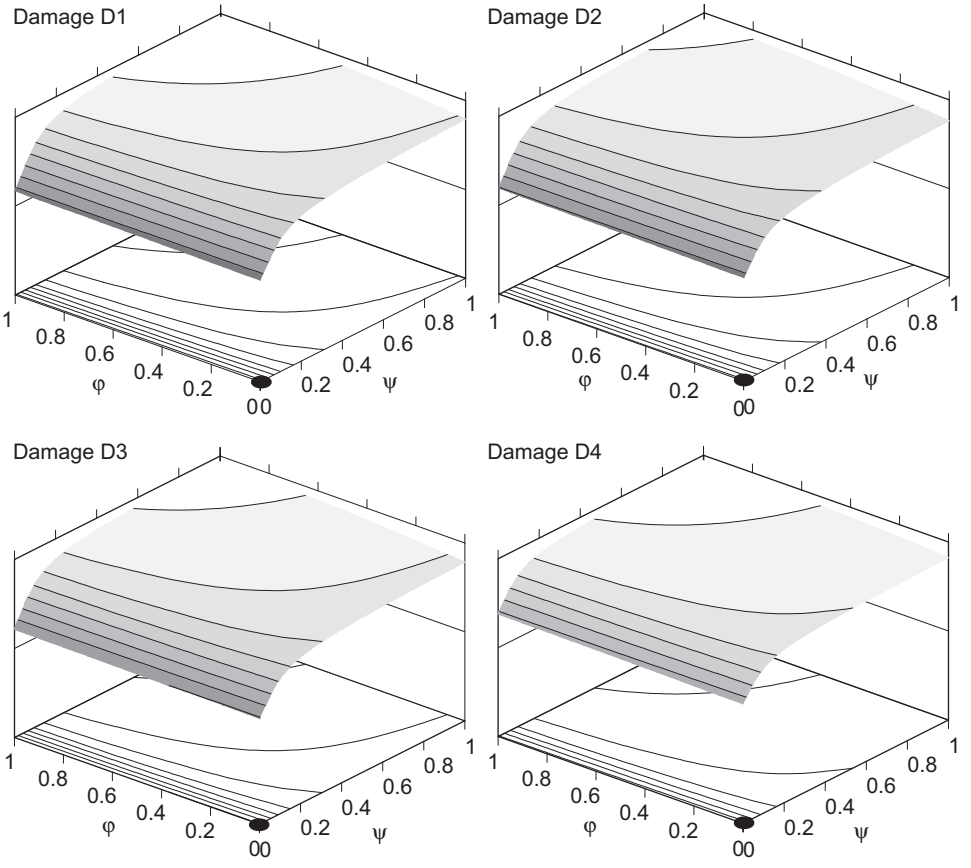

Fig. 10. Typical behaviour of the error function $\ell_1(\varphi,\psi)$ defined in Eq. (15) (T1PR beam, $N=6$).

To be able to deduct the modelling errors in the model calibration, in a second stage the following error function has been introduced:

$$\ell_2(\varphi,\psi)=\sum_{r=1}^{N}\left(\frac{f_{r,\mathrm{exp}}-f^{*}_{r,\mathrm{anal}}(\varphi,\psi)}{f_{r,\mathrm{exp}}}\right)^2,\quad \text{with } f^{*}_{r,\mathrm{anal}}=\frac{f^{U}_{r,\mathrm{exp}}}{f^{U}_{r,\mathrm{anal}}}\cdot f^{*}_{r,\mathrm{anal}}(\varphi,\psi), \tag{17}$$

where $f^{U}_{r,\mathrm{exp}}, f^{U}_{r,\mathrm{anal}}$ are the rth natural experimental and theoretical frequencies of the undamaged beam. In the expression of Eq. (17), the analytical frequencies are weighted by the factor $f^{U}_{r,\mathrm{exp}}/f^{U}_{r,\mathrm{anal}}$, which should take the modelling error effect into account. It is implicitly assumed here that modelling errors, for every frequency, keep themselves uniform for all the damage configurations. The surface error trend is now more regular and single minimum is present for all the cases studied, see, for example, Fig. 11. The optimum point belongs at a quite flat valley of the surface even in the case of light damages, for which, reasonably, one might expect a certain residual modelling error influence any way. In the case of more severe levels of damage, say from the D2 configuration forward, the minimum point is better definite and, generally, tends to arrange close to side $\varphi=0$, see also Table 5.

The error function of Eq. (17), at last, is suggested to define a new variational problem for the following error function:

$$\ell_3(\varphi,\psi)=\sum_{r=1}^{N}\left(\frac{\Delta f_{r,\mathrm{exp}}}{f^{U}_{r,\mathrm{exp}}}-\frac{\Delta f_{r,\mathrm{anal}}(\varphi,\psi)}{f^{U}_{r,\mathrm{anal}}}\right)^2, \tag{18}$$

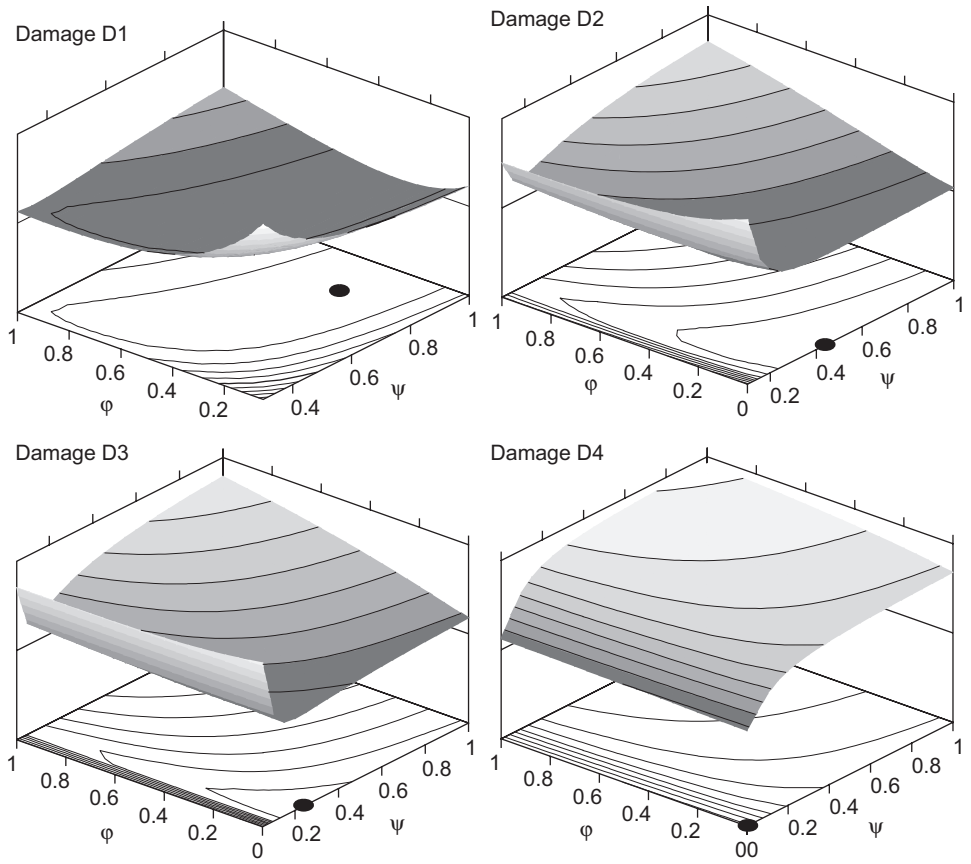

Fig. 11. Typical behaviour of the error function $\ell_2(\varphi,\psi)$ defined in Eq. (17) (T1PR beam, $N=6$).

Table 5
Identified values of shearing, φ, and axial, ψ, damage parameters (Euler–Bernoulli model) based on the optimisation problem of Eq. (17)

Damage	φ			ψ		
	$N=4$	$N=5$	$N=6$	$N=4$	$N=5$	$N=6$
T1PR beam						
D1	0.35	0.35	0.35	1.00	1.00	0.85
D2	0.00	0.00	0.00	0.40	0.50	0.45
D3	0.00	0.00	0.00	0.10	0.20	0.20
D4	0.00	0.00	0.00	0.00	0.00	0.00
T1CR beam						
D1	0.00	0.05	0.15	0.85	1.00	1.00
D2	0.00	0.00	0.00	0.25	0.60	0.95
D3	0.00	0.00	0.00	0.10	0.25	0.40
D4	0.00	0.00	0.00	0.00	0.00	0.00

Damage configurations as in Fig. 4.

where $\Delta f_{r,\mathrm{exp}}$ and $\Delta f_{r,\mathrm{anal}}(\varphi,\psi)$ denote, respectively, the experimental and the analytical value of the *frequency variation* between undamaged and damaged configurations corresponding to the rth mode. This objective function, as in Ref. [6], is not definite any more in terms of the percentage differences between analytical and experimental frequencies, but depends on the *differences of the percentage variations* of the analytical and

experimental changes. In this approach, it is implicitly assumed that the analytical model, even if inaccurate in the absolute estimate of the natural frequencies, is still able to reproduce in a sufficiently careful way the percentage changes of frequency between the undamaged and a damaged configurations. In other words, as frequency changes depend on the frequency sensitivity for small perturbations of the parameters, one is assuming that the model is at least able to carefully estimate the sensitivity of various frequencies. The typical trend of the surface error built with the expression of Eq. (18) is shown, by way of example, in Fig 12. By the analysis of the plots, a certain likeness with the surface built by Eq. (17) clearly emerges. In particular the optimum damage parameter values coincide with those obtained by the variational approach based on the error function of Eq. (17). Moreover, a progressive decrease of the parameters, more marked for φ, is noticed as far as the damage increases. As expected, for the most severe level of damage, corresponding to configuration D4, both the identified coefficients vanish.

Taking into account the above results, in what follows the optimal values of φ, ψ corresponding to the optimisation problem of Eq. (17) (or of Eq. (18)) with $N = 6$ will be considered. With these optimal values for φ and ψ, the first frequencies of the damaged composite beam were estimated and compared to those measured during experiments, see Columns 5–16 of Tables 2 and 3, for T1PR and T1CR beam, respectively. It turns out that the calibrated model is able to accurately reproduce the first natural frequencies for the intermediate damage configurations D1, D2, D3, as well as for the severe damage state D4. The variations of the analytical frequency values are fairly similar to those measured during tests and the percentage modelling errors are almost the same for all the studied configurations. Finally, the model precisely reproduces the experimental flexural modes, see, for example, Figs. 13 and 14 for T1PR beam in damaged configurations D2 and D4, respectively.

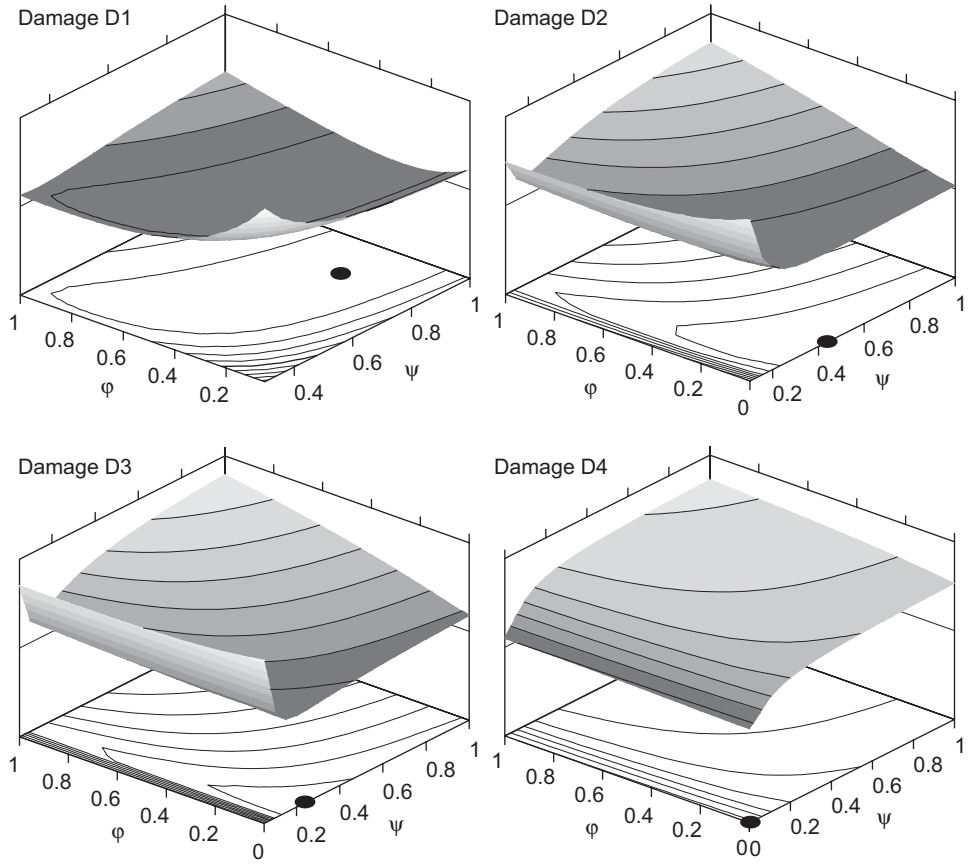

Fig. 12. Typical behaviour of the error function $\ell_3(\varphi, \psi)$ defined in Eq. (18) (T1PR beam, $N = 6$).

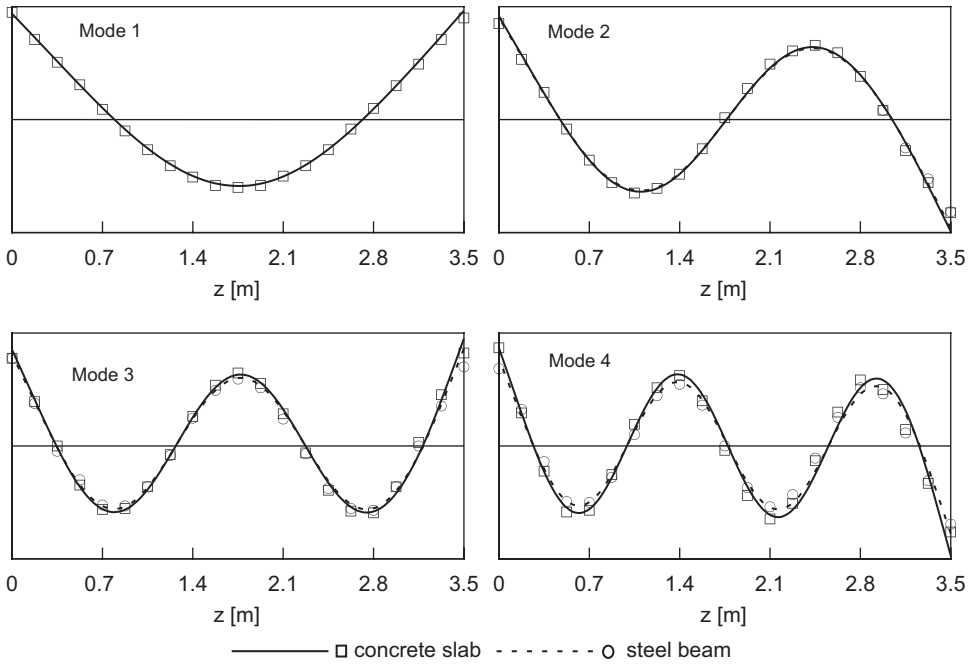

Fig. 13. Comparison between the first four analytical and experimental (dots) flexural modes of T1PR beam in damage configuration D2. Experimental data from Ref. [13].

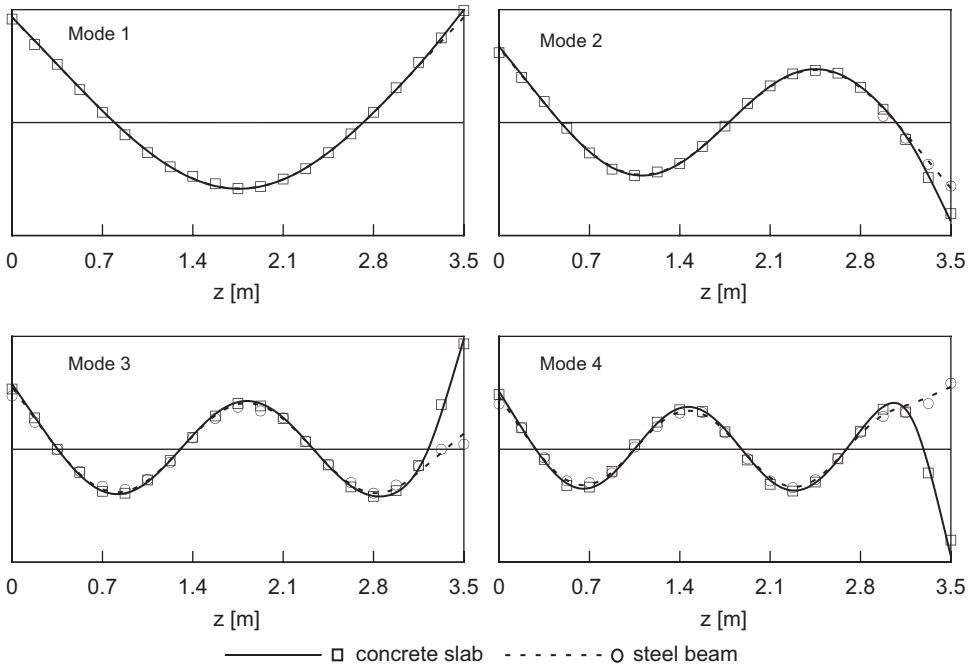

Fig. 14. Comparison between the first four analytical and experimental (dots) flexural modes of T1PR beam in damage configuration D4. Experimental data from Ref. [13].

It can be concluded that the proposed model, suitably calibrated via dynamic data, can be used to accurately describe the actual behaviour of composite beams in flexural vibrations with *severe* and also *intermediate* levels of damage, which is one of the two main aims of the present research. The second

goal concerns damage identification based on frequency shift data. This issue will be discussed in the next section.

4. Damage detection based on shift frequency data

The diagnostic technique which will be used to identify damage is an extension of that presented in Ref. [9] for the localisation of severe damage (corresponding to level D4) in one end connector of a composite beam. The identification of such a damage, roughly speaking, reduces the inverse problem to the *localisation* of the fault, since it is a priori known that the damage stiffness coefficients vanish simultaneously, i.e. $\varphi = \psi = 0$. Assuming that damage is known to affect only one connector and, by symmetry, that it is known beforehand to be located in one-half of the beam (the right one, for example), the inverse diagnostic problem posed in Ref. [9] was the following optimisation problem:

$$\begin{aligned} &\text{to find } \widetilde{z}_i, \widetilde{z}_i \in \{z_1, \ldots, z_p\} \equiv \mathscr{D} \\ &\text{such that } f(\widetilde{z}_i) = \min_{z_k \in \mathscr{D}} \sum_{r=1}^{N} (\Delta f_{r,\mathrm{exp}} - \Delta f_{r,\mathrm{anal}}(z_k))^2, \end{aligned} \tag{19}$$

where $\mathscr{D}$ is the set of possible damage locations. This method allowed the unique localisation of the damage, see Ref. [9].

The situation in the case of *intermediate levels of damage* is significantly different, since the identification involves also the determination of the damage parameters φ and ψ. To solve this diagnostic problem, the approach proposed, for example, in Ref. [6] for assessment of diffuse cracking in a reinforced concrete beam via frequency shifts has been followed. Under the a priori assumption that there is a single damaged connector, a two-step procedure was implemented. In the first step, for a given tentative damage position z_i, the following variational problem was posed:

$$\text{to find } (\widetilde{\varphi}_i, \widetilde{\psi}_i) \text{ such that } \ell_3(z_i, \widetilde{\varphi}_i, \widetilde{\psi}_i) = \min_{(\varphi,\psi)\in[0,1]\times[0,1]} \ell_3(z_i, \varphi, \psi), \tag{20}$$

where $\ell_3(z_i, \varphi, \psi)$ is given as in Eq. (18) for a damaged connector located at $z = z_i$. By solving the problem shown in Eq. (20) for every i ($i = 9, \ldots, 16$, $i = 12, \ldots, 23$ for T1PR and T1CR beams, respectively, see Fig. 3), we obtain

$$\widetilde{\ell}_3(z_i) = \ell_3(z_i, \widetilde{\varphi}_i, \widetilde{\psi}_i), \tag{21}$$

which is now a function of the position variable only. Finally, the solution of the diagnostic problem is given by finding the minimum of $\widetilde{\ell}_3 = \widetilde{\ell}_3(z_i)$ on the finite set of connector positions $\mathscr{D}$, namely:

$$\text{to find } \widetilde{z}_i, \widetilde{z}_i \in \mathscr{D} \text{ such that } \widetilde{\ell}_3(\widetilde{z}_i) = \min_{z_k \in \mathscr{D}} \widetilde{\ell}_3(z_k), \tag{22}$$

where $\mathscr{D} = \{z_9, \ldots, z_{16}\}$, $\mathscr{D} = \{z_{12}, \ldots, z_{23}\}$ for T1PR and T1CR beams, respectively.

The results of the damage identification are shown in Figs. 15 and 16. The plotted functions $\widetilde{\ell}_3$ have been obtained for $N = 4, 5, 6$. Concerning T1PR beam, it can be seen that, starting from damage configuration D2, the absolute minimum of the function $\widetilde{\ell}_3$ in Eq. (21) is well defined and the exact solution is uniquely found. The identification is less clear for T1CR beam, where a significant local minimum of $\widetilde{\ell}_3$ appears around studs 15–17 and 12–17 in damage configurations D2 and D3, respectively. This different behaviour is due to the fact that T1CR beam is obviously less sensitive to a damage in a single connector than T1PR beam and, therefore, modelling errors can more easily mask the frequency changes induced by the damage. As expected, the indication obtained for damage D1 is quite inaccurate, because of the probable perturbation of the specimen caused by execution of the damage.

Finally, once the location $\widetilde{z}_i$ of the damaged stud is identified, the values of $\widetilde{\varphi}_i$, $\widetilde{\psi}_i$ that minimize the error function in Eq. (20) represent an estimate of the level of damage. Obviously, when the damaged stud is properly located (from configuration D2 forward), these values coincide with those collected in Tables 5 and 8.

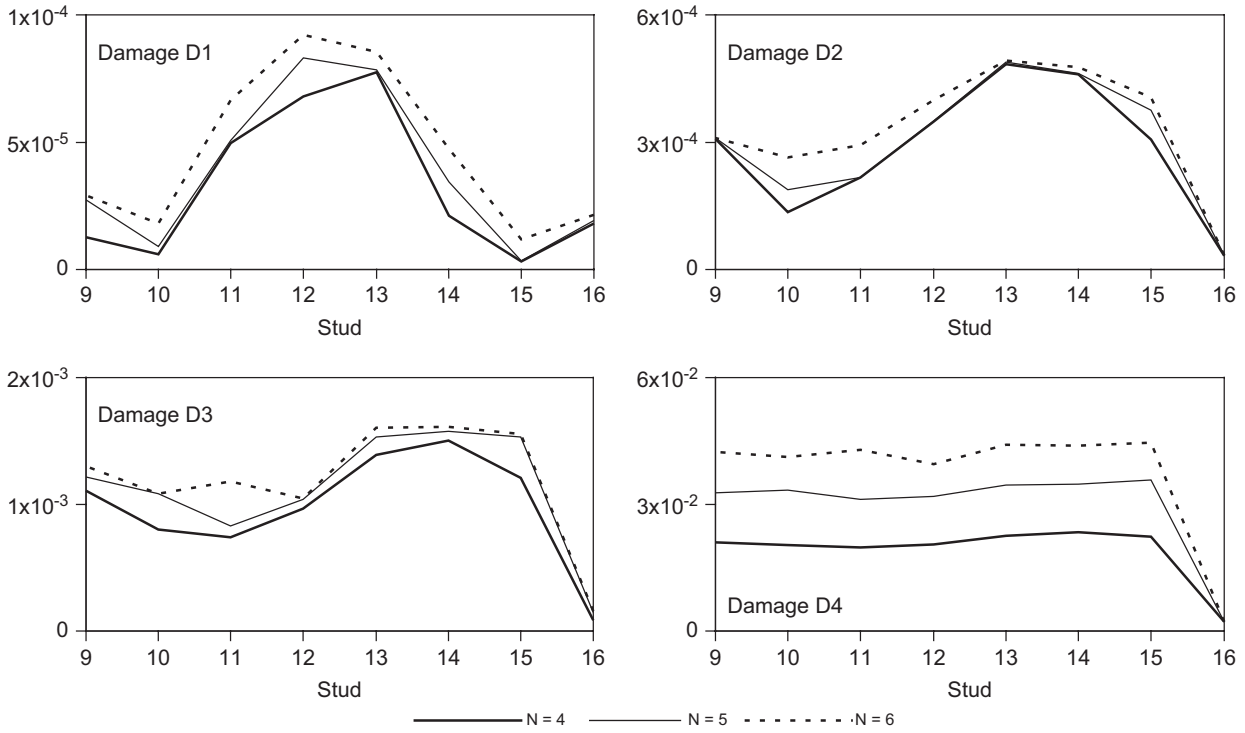

Fig. 15. Damage detection for T1PR beam (Euler–Bernoulli model): error function $\widetilde{\ell}_3 = \widetilde{\ell}_3(z_k)$ for different number of frequencies N and $k = 9, \ldots, 16$. Actual damaged stud: number 16.

5. A Timoshenko analytical model of composite beam

At the end of the previous section, it was shown that damage identification based on Euler–Bernoulli model defined by Eq. (6) is able to locate the damage starting from level D2 only, since modelling errors are too large with respect to the frequency changes induced by very small damages (level D1, in the present case). This aspect is well known in the literature (see also Refs. [11,12]) and it has motivated the introduction of a refined version of the Euler–Bernoulli model developed, namely Timoshenko model of composite beam.

Most of the matter of this analysis follows the lines of Sections 2–4. Therefore, the interested reader is referred to Ref. [23] for more details.

The Timoshenko model includes, in addition to the Euler–Bernoulli one, the influence of shear deformation of the concrete slab and the steel beam, and it also takes into account the rotary inertia of the two beams. Thus, the eigenvalue problem for a free–free composite beam with a damaged end connector is governed by the coupled differential system defined in $(0, L-d) \cup (L-d, L)$:

$$\begin{cases} N_1' + k_d(u_2 - u_1 - e_c\phi_1 - e_s\phi_2) + \omega^2\rho_1 u_1 = 0, \\ N_2' - k_d(u_2 - u_1 - e_c\phi_1 - e_s\phi_2) + \omega^2\rho_2 u_2 = 0, \\ T_1' + \mu_d(v_2 - v_1) + \omega^2\rho_1 v_1 = 0, \\ T_2' - \mu_d(v_2 - v_1) + \omega^2\rho_2 v_2 = 0, \\ M_1' - T_1 + k_d e_c(u_2 - u_1 - e_c\phi_1 - e_s\phi_2) - \omega^2\rho_1 \dfrac{J_1}{A_1}\phi_1 = 0, \\ M_2' - T_2 + k_d e_s(u_2 - u_1 - e_c\phi_1 - e_s\phi_2) - \omega^2\rho_2 \dfrac{J_2}{A_2}\phi_2 = 0 \end{cases} \tag{23}$$

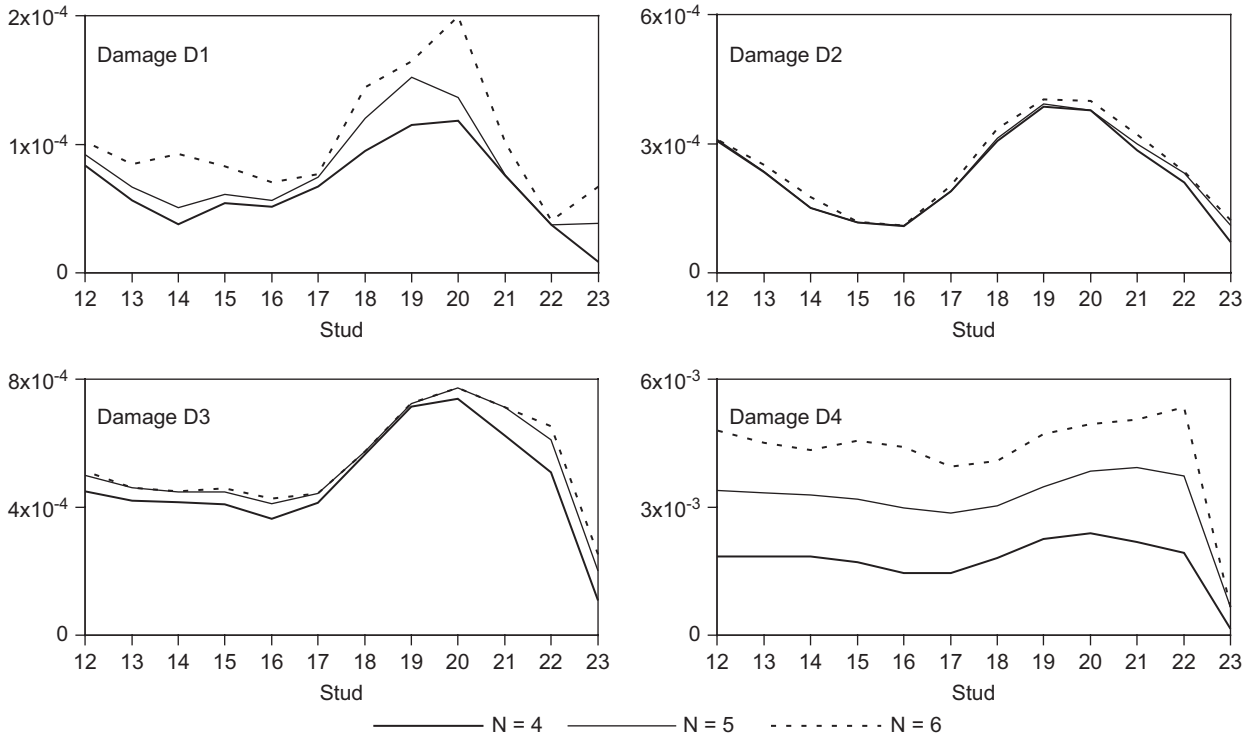

Fig. 16. Damage detection for T1CR beam (Euler–Bernoulli model): error function $\widetilde{\ell}_3 = \widetilde{\ell}_3(z_k)$ for different number of frequencies N and $k = 12, \ldots, 23$. Actual damaged stud: number 23.

with natural boundary conditions

$$N_i(z) = 0, \quad T_i(z) \equiv g_i(z)(v_i'(z) + \phi_i(z)) = 0, \quad M_i(z) \equiv j_i(z)\phi_i'(z) = 0, \tag{24}$$

at $z = 0$ and $z = L$, $i = 1, 2$, and jump conditions

$$\begin{aligned} &[u_i(L-d)] = [v_i(L-d)] = [\phi(L-d)] = 0, \\ &[N_i(L-d)] = [T_i(L-d)] = [M_i(L-d)] = 0, \end{aligned} \tag{25}$$

$i = 1, 2$. In the above equations $g_i \equiv G_i A_i / q_i$ is the shearing stiffness of the ith beam transversal section, $G_i = E_i/2(1 + v_i)$ is the shear modulus, v_i the Poisson coefficient of the ith material, and q_i the shear factor of the ith cross-section. Moreover, $\phi_i = \phi_i(z, t)$ is the rotation angle of the ith cross-section around axis X_i, $i = 1, 2$.

A closed-form solution of the eigenvalue problem of Eqs. (23)–(25) was derived in Ref. [23] for composite beams with stepwise constant coefficients.

The analytical model was defined by means of the same identification procedure used in Section 3 for the Euler–Bernoulli model. Also in the present case, the axial stiffness of the connection was identified by minimizing the error function (12) and the shearing stiffness was determined by imposing the coincidence of the analytical and experimental frequency associated to the fundamental mode. The optimal axial stiffness is slightly less than the value obtained by the Euler–Bernoulli model ($0.40\mu_0$ instead of $0.50\mu_0$), whereas there is a significant change in the shearing stiffness. The optimal value of k is $2.15k_0$ and $3.48k_0$ for beam T1PR and T1CR, respectively. Finally, in the model, the shear factors q_1 and q_2 were assumed, respectively, 1.2 and 2.49, and Poisson's ratios v_1 and v_2 were assumed, respectively, 0.166 and 0.30.

Tables 6 and 7 compare the experimental and the analytical frequencies of T1PR and T1CR beams in undamaged configurations and for damage states D1–D4. Generally speaking, all the first seven frequencies

Table 6
Comparison between experimental and analytical frequencies (Timoshenko model) of flexural vibration modes for T1PR beam in undamaged and damaged configurations (rigid motions are omitted)

Mode	Undamaged			Damage D1			Damage D2			Damage D3			Damage D4		
	Exp.	Anal.	Δ%	Exp.	Anal.	Δ%	Exp.	Anal.	Δ%	Exp.	Anal.	Δ%	Exp.	Anal.	Δ%
1	60.68	60.68	0.0	60.51	60.58	0.1	60.25	60.48	0.4	60.21	60.45	0.4	59.81	60.25	0.7
2	145.46	147.66	1.5	144.08	144.93	0.6	142.70	146.11	2.4	142.18	145.69	2.5	136.76	143.24	4.7
3	247.11	253.75	2.7	245.14	251.71	2.7	241.93	249.24	3.0	238.95	247.58	3.6	222.58	236.53	6.3
4	351.08	369.95	5.4	348.72	366.57	5.1	343.62	362.10	5.4	339.22	358.31	5.6	309.10	332.95	7.7
5	461.38	492.89	6.8	457.49	488.70	6.8	452.41	482.41	6.6	447.98	476.29	6.3	402.96	439.07	9.0
6	570.77	620.95	8.8	565.91	616.21	8.9	560.31	608.79	8.7	554.64	600.85	8.3	503.66	554.91	10.2
7	691.48	754.31	9.1	686.11	749.79	9.3	679.84	741.67	9.1	673.37	732.44	8.8	599.82	672.43	12.1

Identified values of the damaged parameters φ and ψ as in Table 8. $\Delta\% = 100(f_{\text{anal}} - f_{\text{exp}})/f_{\text{exp}}$. Frequency values in Hertz. Experimental data from Ref. [13].

Table 7
Comparison between experimental and analytical frequencies (Timoshenko model) of flexural vibration modes for T1CR beam in undamaged and damaged configurations (rigid motions are omitted)

Mode	Undamaged			Damage D1			Damage D2			Damage D3			Damage D4		
	Exp.	Anal.	Δ%	Exp.	Anal.	Δ%	Exp.	Anal.	Δ%	Exp.	Anal.	Δ%	Exp.	Anal.	Δ%
1	60.49	60.49	0.0	60.37	60.46	0.2	60.30	60.45	0.3	60.29	60.44	0.2	60.24	60.36	0.2
2	146.34	152.04	3.9	145.12	151.71	4.5	144.80	151.57	4.7	143.97	151.42	5.2	144.30	150.37	4.2
3	250.82	266.34	6.2	248.18	265.11	6.8	246.05	264.54	7.5	245.60	263.89	7.4	242.46	258.77	6.7
4	361.26	391.16	8.3	357.09	388.51	8.8	356.18	387.13	8.7	353.42	385.46	9.1	346.21	371.16	7.2
5	473.88	521.11	10.0	471.08	516.85	9.7	468.90	514.43	9.7	466.29	511.38	9.7	451.06	485.43	7.6
6	588.38	654.48	11.2	586.28	648.80	10.7	583.34	645.36	10.6	580.71	640.99	10.4	560.88	609.50	8.7
7	709.04	791.41	11.6	708.14	784.69	10.8	703.65	780.46	10.9	700.58	775.15	10.6	668.07	735.39	10.1

Identified values of the damaged parameters φ and ψ as in Table 8. $\Delta\% = 100(f_{\text{anal}} - f_{\text{exp}})/f_{\text{exp}}$. Frequency values in Hertz. Experimental data from Ref. [13].

are overestimated, with percentage errors less than half of those corresponding to the Euler–Bernoulli model, see Columns 2–4 of Tables 6 and 7. These results confirm the trend already observed in Ref. [14].

The identification procedure illustrated in Section 3 for the calibration of the model in case of damage was repeated for Timoshenko model. Poor results were obtained, as before, when the variational identification is based on the error function (16). Conversely, the use of the error functions (17) or (18) allowed for a unique and rather stable identification of the damage parameters φ and ψ. The optimal values obtained by the two methods are practically coincident and are collected in Table 8. As in the Euler–Bernoulli model, the shearing stiffness vanishes starting from damage configuration D2, whereas the axial stiffness shows more gradual reductions for increasing damage and it turns out to be slightly affected by the number N of frequencies used. Measured and calculated frequencies for all damaged configurations are compared in Columns 5–16 of Tables 6 and 7 (for $N = 6$). Modelling errors are similar to those observed in the undamaged configuration and, in general, Timoshenko model enhances the accuracy in describing the dynamic behaviour of the composite system. A comparison of the first flexural modes shows a good agreement between experimental findings and analytical estimates.

The damage identification method presented in the previous section has been applied on the basis of the Timoshenko model. The final results are shown in Figs. 17 and 18. It can be observed that the Timoshenko model slightly improves the accuracy of the identification, although localization of damage D1 still remains somewhat uncertain.

For the sake of completeness, the damage identification technique was also applied to a Timoshenko model in which the values of the axial and shearing stiffness of the undamaged beam were taken coincident with

Table 8
Identified values of shearing, φ, and axial, ψ damage parameters (Timoshenko model), based on the optimisation problem of Eq. (17)

Damage	φ			ψ		
	$N=4$	$N=5$	$N=6$	$N=4$	$N=5$	$N=6$
T1PR beam						
D1	0.25	0.25	0.25	1.00	1.00	1.00
D2	0.00	0.00	0.00	0.30	0.35	0.40
D3	0.00	0.00	0.00	0.10	0.15	0.15
D4	0.00	0.00	0.00	0.00	0.00	0.00
T1CR beam						
D1	0.00	0.00	0.05	0.30	0.70	1.00
D2	0.00	0.00	0.00	0.15	0.30	0.50
D3	0.00	0.00	0.00	0.10	0.15	0.25
D4	0.00	0.00	0.00	0.00	0.00	0.00

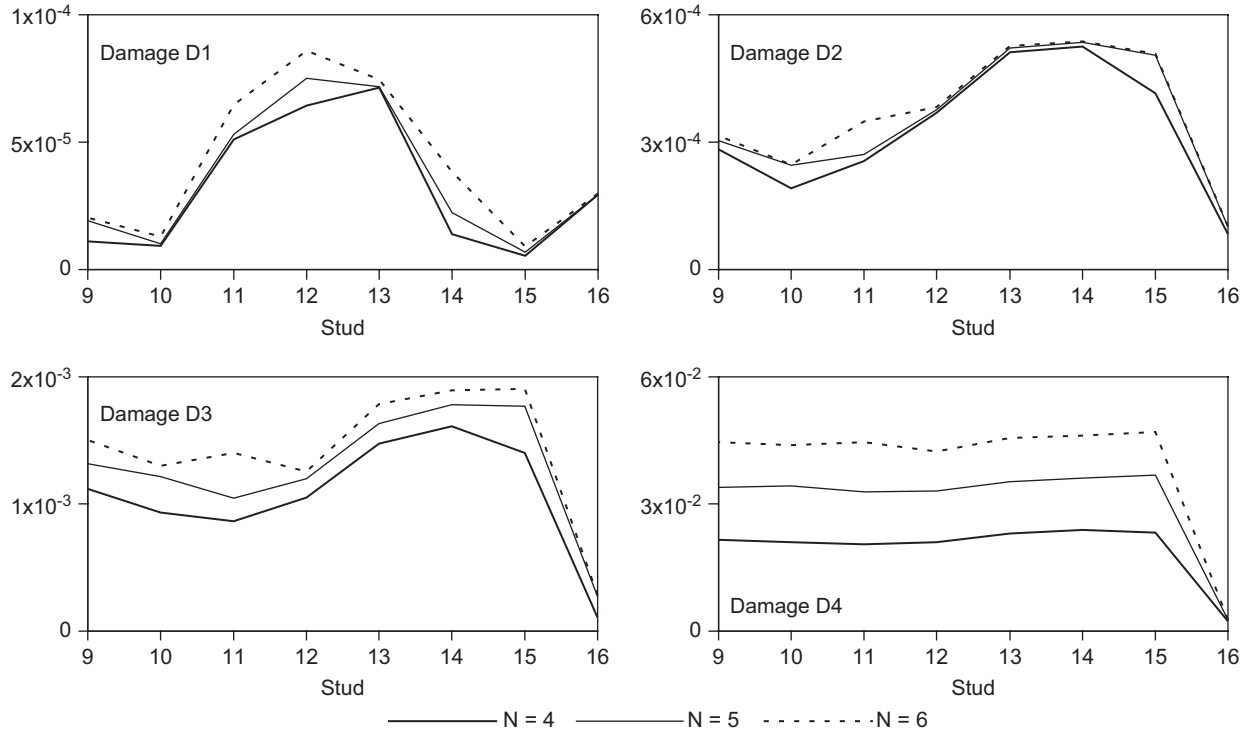

Fig. 17. Damage detection for T1PR beam (Timoshenko model): error function $\widetilde{\ell}_3 = \widetilde{\ell}_3(z_k)$ for different number of frequencies N and $k = 9, \ldots, 16$. Actual damaged stud: number 16.

those found in the Euler–Bernoulli model. Without going into details, this analytical model underestimates by about 1.9% and 2.0% the fundamental frequency, respectively, for undamaged T1PR and T1CR beams. The second and the third frequencies are also slightly underestimated, by about 2.7% and 1.9%, and 1.3% and 0.7%, for T1PR and T1CR beams, respectively, whereas high-order frequencies are overestimated, with percentage errors which increase with the order of the mode up to 8% for the seventh vibration mode. Taking into account the underestimate of the fundamental frequency and considering that large changes in the shearing stiffness produce small absolute variations of the fundamental frequency, incidentally one can explain the large changes obtained in estimating k by imposing the coincidence of the analytical and the

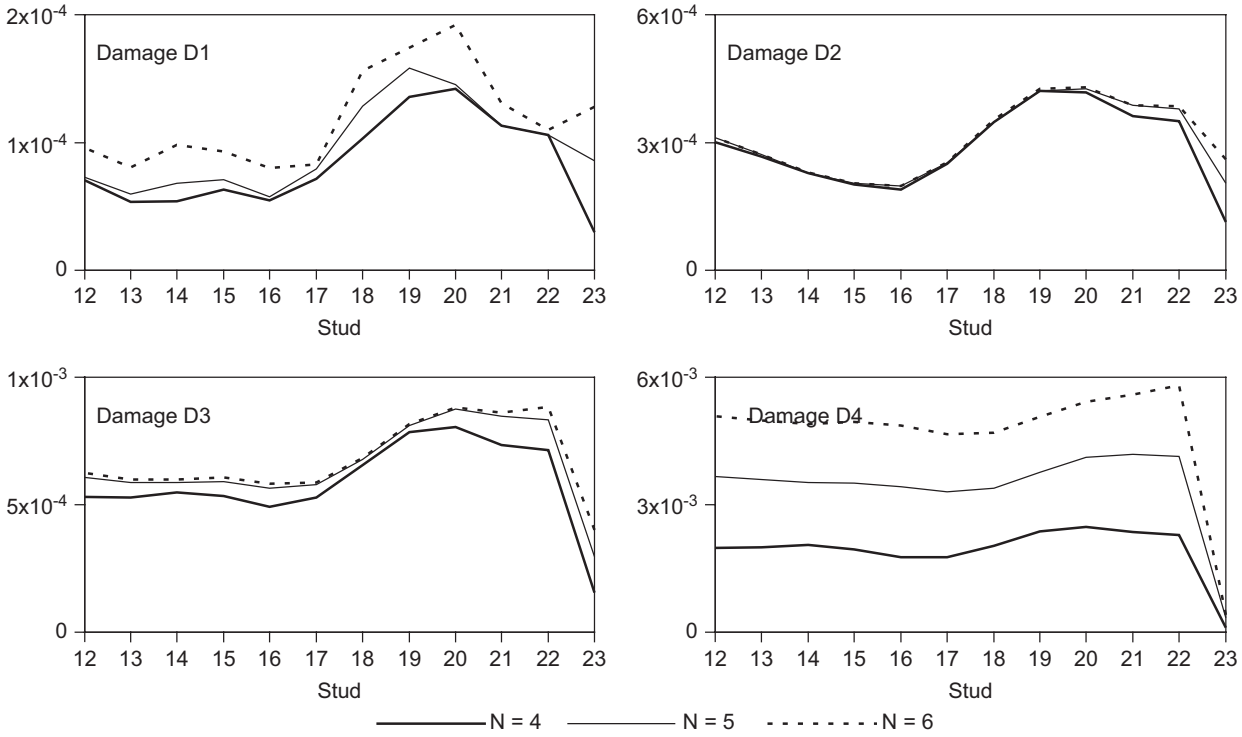

Fig. 18. Damage detection for T1CR beam (Timoshenko model): error function $\widetilde{\ell}_3 = \widetilde{\ell}_3(z_k)$ for different number of frequencies N and $k = 12, \ldots, 23$. Actual damaged stud: number 23.

experimental frequencies associated to the fundamental mode. Finally, one can show that with this definition of the Timoshenko model of the undamaged beam, the final results of damage identification remain virtually unchanged. This suggests that the proposed damage identification technique has a certain degree of stability to slightly different choices of analytical model used in interpreting the measurements.

6. Conclusions

In this paper an Euler–Bernoulli model with a shearing-type strain energy of the connection has been proposed to describe the dynamic behaviour of steel–concrete composite beams in undamaged configuration and with partially degraded connection. In the experiments, the damage was simulated by means of a crack of increasing depth produced on one end connector.

The mechanical model has been calibrated on the basis of dynamic tests carried out on specimens. Analytical values of modal parameters, such as natural frequencies and mode shapes, show a good agreement with measurements and a uniform degree of accuracy for all the damage configurations is observed. The accuracy in reproducing the experimental data has been further improved by introducing a Timoshenko-type model for the composite beam.

The two models have been used to detect damage by means of a variational-type method based on frequency shift measurements only. Good indication, both for damage location and severity, has been obtained when the first few flexural frequencies are included in identification. This shows that the frequency variations contain information on the position of the damage. It should be noted, however, that all results presented in this article are based on damage located at the ends of the composite beam. When the damage is located in an internal connector, dynamic tests conducted by Biscontin and Wendel [24] and numerical simulations carried out in Ref. [9], show that the variations in frequency are less than those induced by damage in an ending stud. Therefore, it would be important to test the sensitivity of the proposed technique for the

identification of these damage scenarios. As a first step, the development of an experimental research, such as that presented in Ref. [13], on this issue would be highly desirable.

Other diagnostic methods based on dynamic data have been recently proposed to identify damage in steel–concrete composite beams. Xia et al. [3] introduced a damage index based on frequency response function measurements taken both on the slab and on the beams for damage detection in slab-girder bridges. Their method has a local character and has been applied to the study of a scaled bridge model built in laboratory. In Ref. [25] it was proved that the shearing stiffness coefficient can be uniquely reconstructed from the frequency response function of the composite beam evaluated at one end of the beam, under the assumption that only longitudinal motions are present. An extension of the above results has been obtained in Ref. [26] when measurements are taken at both the ends of the beam. The full coupled vibrational problem, which includes both flexural and axial motions, has been examined in Ref. [27]. A variational procedure based on dynamical measurements taken at the boundary and, possibly, at some interior portions of the beam was proposed and used for the identification of the shearing and axial stiffness of the connection. The encouraging results found in Ref. [27] and the appreciable sensitivity to damage of flexural mode shapes shown in Ref. [13], suggest that variational methods based on both natural frequencies and modal components may be useful to improve the results of damage detection techniques on steel–concrete composite structures. This seems to be another promising direction for further research on this field.

References

[1] G. Biscontin, A. Morassi, P. Wendel, Vibrations of steel–concrete composite beams, *Journal of Vibration and Control* 6 (2000) 691–714.

[2] R.P. Johnson, *Composite Structures of Steel and Concrete*, Blackwell Scientific, Oxford, UK, 1994.

[3] Y. Xia, H. Hao, A.J. Deeks, Dynamic assessment of shear connectors in slab-girder bridges, *Engineering Structures* 29 (7) (2007) 1475–1486.

[4] G. Hearn, R.B. Testa, Modal analysis for damage detection in structures, *ASCE Journal of Structural Engineering* 117 (10) (1991) 3042–3063.

[5] R.Y. Liang, J. Hu, F. Choy, Quantitative NDE technique for assessing damages in beam structures, *ASCE Journal of Engineering Mechanics* 118 (7) (1992) 1468–1487.

[6] M.N. Cerri, F. Vestroni, Use of frequency change for damage identification in reinforced concrete beams, *Journal of Vibration and Control* 9 (2003) 475–491.

[7] A. Morassi, Damage detection and generalized Fourier coefficients, *Journal of Sound and Vibration* 302 (2007) 229–259.

[8] A. Morassi, L. Rocchetto, A damage analysis of steel–concrete composite beams via dynamic methods, Part I: experimental results, *Journal of Vibration and Control* 9 (5) (2003) 507–527.

[9] M. Dilena, A. Morassi, A damage analysis of steel–concrete composite beams via dynamic methods, Part II: analytical models and damage detection, *Journal of Vibration and Control* 9 (5) (2003) 529–565.

[10] C. Davini, F. Gatti, A. Morassi, A damage analysis of steel beams, *Meccanica* 28 (1993) 27–37.

[11] C. Davini, A. Morassi, N. Rovere, Modal analysis of notched bars: tests and comments on the sensitivity of an identification technique, *Journal of Sound and Vibration* 179 (3) (1995) 513–527.

[12] A. Morassi, N. Rovere, Localizing a notch in a steel frame from frequency measurements, *ASCE Journal of Engineering Mechanics* 123 (5) (1997) 422–432.

[13] M. Dilena, A. Morassi, Experimental modal analysis of steel–concrete composite beams with partially damaged connection, *Journal of Vibration and Control* 10 (2004) 897–913.

[14] S. Berczynski, T. Wróblewski, Vibration of steel–concrete composite beams using the Timoshenko beam model, *Journal of Vibration and Control* 11 (2005) 829–848.

[15] N.M. Newmark, C.P. Siess, I.M. Viest, Tests and analysis of composite beams with incomplete interaction, *Proceedings of the Society of Experimental Stress Analysis* 9 (1951) 75–92.

[16] A.O. Adekola, Partial interaction between elastically connected elements of a composite beam, *International Journal of Solids and Structures* 4 (1968) 1125–1135.

[17] P. Ansourian, J.W. Roderick, Analysis of composite beams, *ASCE Journal of Structural Division* 104 (10) (1978) 1631–1645.

[18] V. Kristek, J. Studnicka, Analysis of composite girders with deformable connectors, *Proceedings of the Institution of Civil Engineers* 73 (2) (1982) 699–712.

[19] P. Gelfi, E. Giuriani, Theoretical constitutive law for stud shear connectors, *Studi e Ricerche* 9 (1987) 323–341.

[20] R. Betti, A. Gjelsvik, Elastic composite beams, *Computer & Structures* 59 (3) (1996) 437–451.

[21] N. Gattesco, Analytical modeling of nonlinear behavior of composite beams with deformable connection, *Journal of Constructional Steel Research* 52 (2) (1999) 195–218.

[22] H.F. Weinberger, *A First Course in Partial Differential Equations*, Dover Publications Inc., New York, 1965.

[23] M. Dilena, Modal Analysis and Damage Detection of Steel–concrete Composite Beams, Ph.D. Thesis, University of Bologna, Italy, 2006.
[24] G. Biscontin, P. Wendel, Structural Diagnostics of Steel–concrete Composite Beams via Dynamic Methods, Engng. Thesis, University of Udine, Italy, 1998.
[25] A. Morassi, G. Nakamura, M. Sini, An inverse dynamical problem for connected beams, *European Journal of Applied Mathematics* 16 (2005) 83–109.
[26] M.I. Belishev, S.A. Ivanov, Recovering the parameters of the system of connected beams from dynamical boundary measurements, *Zapiski Nauchnykh Seminarov POMI* 324 (2005) 20–42 (in Russian).
[27] A. Morassi, G. Nakamura, K. Shirota, M. Sini, A variational approach for an inverse dynamical problem for composite beams, *European Journal of Applied Mathematics* 18 (1) (2007) 21–55.